PAPER

CrossMark
click for updates

Aqueous biphasic systems composed of ionic liquids and polypropylene glycol: insights into their liquid–liquid demixing mechanisms†

Catarina M. S. S. Neves,‡[a] Shahla Shahriari,‡[ab] Jesus Lemus,[a] Jorge F. B. Pereira,[c] Mara G. Freire[a] and João A. P. Coutinho*[a]

Novel ternary phase diagrams of aqueous biphasic systems (ABSs) composed of polypropylene glycol with an average molecular weight of 400 g mol^{-1} (PPG-400) and a vast number of ionic liquids (ILs) were determined. The large array of selected ILs allowed us to evaluate their tuneable structural features, namely the effect of the anion nature, cation core and cation alkyl side chain length on the phase behaviour. Additional evidence on the molecular-level mechanisms which rule the phase splitting was obtained by ^{1}H NMR (Nuclear Magnetic Resonance) spectroscopy and by COSMO-RS (Conductor-like Screening Model for Real Solvents). Some systems, for which the IL–PPG-400 pairs are completely miscible, revealed to be of type "0". All data collected suggest that the formation of PPG–IL-based ABSs is controlled by the interactions established between the IL and PPG, contrarily to previous reports where a "salting-out" phenomenon exerted by the IL over the polymer in aqueous media was proposed as the dominant effect in ABS formation. The influence of temperature on the liquid–liquid demixing was also evaluated. In general, an increase in temperature favours the formation of an ABS in agreement with the lower critical solution temperature (LCST) phase behaviour usually observed in polymer–IL binary mixtures. Partition results of a dye (chloranilic acid, in its neutral form) further confirm the possibility of tailoring the phases' polarities of IL–PPG-based ABSs.

Introduction

In recent years, ionic liquids (ILs) have become the subject of widespread academic studies as potential substitutes of common molecular organic solvents.[1,2] They are a class of molten salts in which their ions are poorly coordinated, and thus are, by general definition, liquid at temperatures below 100 °C. The unique characteristics of most of these liquid salts, namely negligible vapour pressure, high thermal and chemical stabilities and non-flammability, make them interesting solvents for a wide variety of applications. These applications comprise their

[a] CICECO – Aveiro Institute of Materials, Department of Chemistry, University of Aveiro, 3810-193 Aveiro, Portugal. E-mail: jcoutinho@ua.pt
[b] Department of Chemical Engineering Shahr-e-Qods Branch, Islamic Azad University, Tehran, Iran
[c] Department of Bioprocess and Biotechnology, School of Pharmaceutical Sciences, UNESP – Univ Estadual Paulista, Rodovia Araraquara-Jaú/Km 01, Campos Ville, 14800-903 Araraquara, SP, Brazil
† Electronic supplementary information (ESI) available: Experimental weight fraction data for the binodal curves; TLLs, and the percentage weight fraction compositions of PPG and IL in the top and bottom phases; partition coefficients (*K*) of chloranilic acid; pH and conductivity values of both top and bottom phases; σ-profile representation of PPG-400. See DOI: 10.1039/c6cp04023c
‡ Equally contributing authors.

use in catalysis, organic synthesis, electrochemistry, analytical chemistry and extraction and separation processes.[3–6] When dealing with separation processes, one of the paramount properties of ILs is their solvation ability and versatility.[7] The tuneable structures of ILs allow their solvatochromic parameters, namely dipolarity/polarizability and hydrogen-bonding acidity and basicity, to be tailored to a specific task, and to improve the efficiency of separation processes.[8,9]

Ternary systems composed of water-miscible ILs, inorganic/organic salts and water, known as IL-based aqueous biphasic systems (ABSs), have been proposed in the last decade, mainly for use in liquid–liquid extraction.[10,11] Conventional ABSs are formed when two different polymers, or a polymer and a salt, are combined in adequate concentrations in aqueous media causing the system to separate into two aqueous-rich liquid phases.[12] These systems were proposed as alternative platforms for the extraction and purification of biological materials, such as cells, virus, organelles, nucleic acids, amino acids, and proteins, among others.[12] However, recent advances have shown that IL-based ABSs are by far more fascinating than these conventional systems due to the possibility of adapting their phase polarities to maximize the partition and selectivity of target compounds.[13] Indeed, ABSs composed of ILs proved to lead to

This journal is © the Owner Societies 2016

Phys. Chem. Chem. Phys., 2016, **18**, 20571–20582 | 20571

complete extractions of the most diverse compounds, in a single-step, by a proper tuning of their chemical structures.[14–16]

In the past decade, extended investigations on ABSs composed of ILs and inorganic/organic salts, aiming at understanding the mechanisms which rule the liquid–liquid demixing, have been conducted.[10,11,17–21] For all these systems, it was demonstrated that the tendency for liquid–liquid phase separation is related to the ability of the inorganic salt ions to form hydration complexes and to further induce the salting-out of ILs from aqueous media.[17–21] More recently, using a large number of salts, it was established that the salt ions' abilities to induce the formation of IL-based ABSs follow the Hofmeister series and that their molar entropy of hydration is the driving force for the formation of two-phase systems.[22]

In addition to the large number of studies addressing the formation of IL-ABSs by the combination of ILs and salts as phase-forming agents, IL-based ABSs can also be created with polymers, namely polyethylene glycol (PEG)[23–25] and polypropylene glycol (PPG).[26–32] It has been shown that the mechanisms behind the formation of ABSs containing ILs and PEG are far more complex than those observed in salt–IL systems, and depend not only on the IL/salt ions' hydration ability, but also on the interactions occurring between the ionic fluid and the polymer.[24] The influence of favourable IL–PEG interactions on the formation of ABSs was first experimentally observed and later on confirmed by molecular dynamics (MD) simulations.[33,34] Previous research studies on IL–polymer binary systems have demonstrated their organization or ordering.[35,36] Triolo et al.,[35] by small-angle neutron scattering (SANS) studies, concluded that 1-butyl-3-methylimidazolium tetrafluoroborate behaves as an enhanced solvent for PEG, which organizes in the IL in non-entangled random coils. Sarkar et al.[37,38] studied the solvatochromic parameters of mixtures composed of PEGs and 1-butyl-3-methyl-imidazolium hexafluorophosphate. The dipolarity/polarizability and the hydrogen bond acidity of binary mixtures were found to be higher than those predicted from an ideal behaviour, whereas the hydrogen bond basicity was found to fall below.[28] This "anomalous" behaviour was explained based on an extensive hydrogen-bonding network involving the most acidic hydrogen at the C2 position of the imidazolium ring and the terminal hydroxyl as well as the ethoxy groups of PEG (as proton acceptors), and between the IL anion and the terminal hydroxyl groups of PEG.[37,38] In general, all these studies[22,24,34–38] support the existence of a high affinity between polymers and ILs, which is mainly dependent on the polymer nature and on the chemical structure of the IL ions, and further studies have demonstrated that additional interactions between all phase-forming agents in polymer–IL–water ABSs should be considered.[23,39] These works[23,39] revealed that a balance of the cation–PEG, anion–PEG, cation–anion, water–anion, and cation–water interactions, with different relative intensities depending on the phase diagram region, rules the phase-separation mechanism. Thus, and contrarily to previously reported,[24] IL–PEG ABS formation is a result of the preferential solvation of the ether groups in the polymer chain, as well as of the high hydrogen bonding capability of the terminal chain groups of PEG to interact with IL anions or water.[39]

From these previous works,[23,33,34,39] the molecular mechanisms ruling the formation of PEG–IL-based ABSs seem now to be understood; yet, additional works have been reported regarding the capability of PPG to act as a phase-forming agent of ABSs when mixed with aqueous solutions of ILs.[26–32] For these, the mechanisms which govern their phase formation were related to the salting-out ability of ILs and to their "kosmotropic/chaotropic" character.[26–32] However, in all these studies, few ILs were studied (mainly the effect of the IL anion was investigated), and thus, a generalized picture of the molecular-level phenomena responsible for the two-phase formation could not be depicted.[26–30,32] On the other hand, the main aim of some of these works was to demonstrate their performance as extraction systems for amino acids[27] and proteins,[28,30,32] and not to address the molecular-level mechanisms which rule the phase separation.

PPG is more hydrophobic than PEG, which leads to higher interest to explore and understand the liquid–liquid demixing scenario occurring in PPG–IL-based ABSs. PPGs of low molecular weights are completely soluble in water and allow their use as phase-forming constituents of ABSs. As PEG, the attractive properties of PPG are almost null toxicity, negligible volatility, low melting point, low cost and high biodegradability.[28]

This work is focused on providing a comprehensive understanding of the mechanisms which rule the formation of ABSs formed by PPG and ILs. As a first approach, the ternary phase diagrams of PPG-400 with a large array of ILs were determined at 298 K. For some systems, the complete phase diagrams were determined allowing us to demonstrate that they are of type "0", i.e. the pairs IL–PPG, IL–water and PPG–water are completely miscible, yet are able to form two-phase systems at given compositions of the ternary mixtures. The selected ILs, whose chemical structures are shown in Table 1, allowed us to gather ample insights into the influence of their structural features (cation core, anion nature and alkyl side chain length) on the phase diagram behaviour. To further delve into the molecular interactions that govern the formation of IL–PPG ABSs, ^{1}H NMR spectroscopy and COSMO-RS were used. In a second step, the phase diagrams of specific systems at different temperatures (298, 308 and 318 K) were determined to infer on the effect of temperature on their liquid–liquid demixing ability. Finally, the partition coefficients of chloranilic acid between the coexisting phases of several ABSs investigated were determined to evaluate the phases' relative hydrophobicities.

Results and discussion

Ternary phase diagrams

Only a limited number of ILs as ABS phase-forming compounds with PPG was previously evaluated.[26–32] Based on these preliminary results, and aiming at studying the molecular-level mechanisms of ABS formation, we began our investigation by enlarging the number of ILs used to induce PPG-based ABS formation. In this context, a large array of ILs was selected to evaluate the influence of the anion nature, the cation core and

20572 | Phys. Chem. Chem. Phys., 2016, 18, 20571–20582

This journal is © the Owner Societies 2016

Table 1 Chemical structure of the studied ILs and their ability to form ABSs with PPG-400

ILs able to form ABSs with PPG-400			ILs not able to form ABSs with PPG-400		
IL abbreviation[a]	Cation	Anion	IL abbreviation[a]	Cation	Anion
[C₄mim][DMP]			[C₄mim][C₂H₅SO₄]		
[C₄mim][CH₃CO₂]			[C₄mim][CF₃SO₃]		
[C₄mim][CH₃SO₄]			[C₄mim][N(CN)₂]		
[C₄mim]Br		Br⁻	[C₄mim][SCN]		
[C₁mim]Cl		Cl⁻	[C₅mim]Cl		Cl⁻
[C₂mim]Cl		Cl⁻	[C₆mim]Cl		Cl⁻
[C₃mim]Cl		Cl⁻	[C₇mim]Cl		Cl⁻
[C₄mim]Cl		Cl⁻	[N₄₄₄₄]Cl		Cl⁻
[C₄C₁mim]Cl		Cl⁻	[P₄₄₄₄]Cl		Cl⁻
[C₄mpip]Cl		Cl⁻			
[C₄mpy]Cl		Cl⁻			
[C₄mpyr]Cl		Cl⁻			
[Ch]Cl		Cl⁻			

[a] The definition of the IL abbreviations is given in the Experimental section.

the alkyl side chain length at the cation. The IL chemical structures are shown in Table 1, as well as their ability, or not, to form ABSs with PPG-400 at 298 K.

Phase diagrams for ternary mixtures composed of water, PPG-400 and a large set of ILs were determined at 298 K and at atmospheric pressure. To eliminate the effect of the IL molecular weight on the phase diagram representation, binodal curves are compared in molality units (mole of PPG per kg of solvent (water + IL) versus mole of IL per kg of solvent (water + PPG)). All experimental weight fraction data are provided in the ESI.†

In this type of ABS, an aqueous phase rich in IL and water and other mainly composed of polymer and water will be created, where the bottom phase is the IL-rich while the PPG-rich phase corresponds to the top phase.

As stated before, a wide variety of ILs were investigated. The gathered data indicate that some ILs are capable of forming two aqueous phases in the presence of the polymer whereas others are not. Amongst the ILs tested, the following were found to be not able to form ABSs with PPG-400: tetrabutylammonium chloride ([N₄₄₄₄]Cl), tetrabutylphosphonium chloride ([P₄₄₄₄]Cl), 1-butyl-3-methylimidazolium ethylsulphate ([C₄mim][C₂H₅SO₄]), 1-butyl-3-methylimidazolium trifluoromethanesulfonate ([C₄mim]-[CF₃SO₃]), 1-butyl-3-methylimidazolium dicyanamide ([C₄mim]-[N(CN)₂]), 1-butyl-3-methylimidazolium thiocyanate ([C₄mim][SCN]), 1-butyl-3-pentylimidazolium chloride ([C₅mim]Cl), 1-hexyl-3-methylimidazolium chloride ([C₆mim]Cl) and 1-heptyl-3-methyl-imidazolium chloride ([C₇mim]Cl). More hydrophobic ILs and/or ILs composed of ions with a more delocalized charge are not capable of inducing the formation of ABSs with PPG-400. As the ILs are more hydrophobic, their ions hydration in solution is reduced, and consequently present a low capability to dehydrate the moderately hydrophobic polymer. Furthermore, and as previously observed with PEG–IL-based ABSs,[23,24,33,34,39] specific interactions between the polymer and the ILs' ions also occur, dictating not only the phase diagram behaviour, but also the ability to induce, or not, phase splitting.
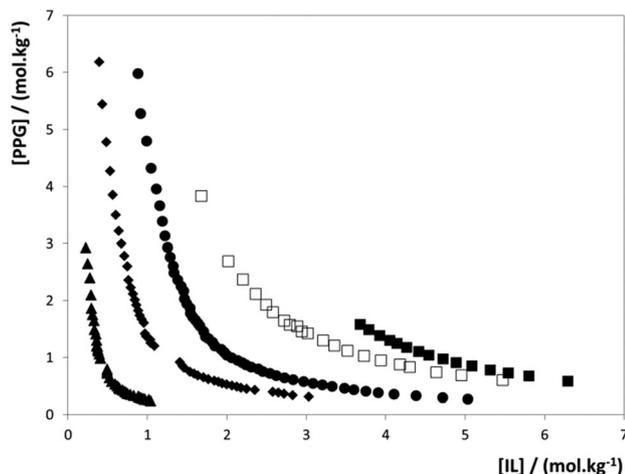
Fig. 1 Binodal curves for ABSs composed of PPG-400 and [C4mim]-based ILs at 298 K: ■, [C4mim]Br; □, [C4mim][CH3SO4]; ●, [C4mim]Cl; ◆, [C4mim][CH3CO2]; ▲, [C4mim][DMP].

Anion nature effect

Since the ability of ILs to promote a two-phase region with PPG in aqueous media must be dominated by their ion nature, we will present and discuss the gathered results by different effects. We start by evaluating the effect of the IL anion by the analysis of the phase diagrams obtained for the [C4mim]-based series of ILs depicted in Fig. 1.

The larger the two-phase region is, *i.e.*, the closer the binodal curve is to the axis, the higher the IL ability to form ABSs. From the data collected, the ability of the IL anion to induce liquid–liquid demixing follows the order: $Br^- < [CH_3SO_4]^- < Cl^- < [CH_3CO_2]^- < [DMP]^-$, with the ILs composed of the anions $[C_2H_5SO_4]^-$, $[CF_3SO_3]^-$, $[N(CN)_2]^-$, and $[SCN]^-$ being unable to form ABSs with PPG-400. This sequence is essentially the opposite to that observed with ABSs formed by ILs and high charge density salts where, amongst the studied ILs, $[C_4mim][CF_3SO_3]$ is in general one of the ILs more prone to undergo phase separation.[18] The trend obtained closely follows the mutual miscibility results provided by Watanabe and co-workers,[40] in which ILs with highly basic/polar anions, such as $[CH_3CO_2]^-$ and $[CH_3SO_3]^-$, are immiscible with the studied polymers, whereas less basic/polar anions, such as $[CF_3SO_3]^-$, are completely miscible at temperatures ranging from room temperature up to 473 K. Accordingly, ILs displaying weaker hydrogen-bond basicity, and thus with lower ability to accept protons, are those that are unable to form ABSs with PPG-400.

The reversed sequences observed in IL + salt[10,11,17–21] and IL + PPG[26–30,32] ABSs were previously rationalized by assuming that, in each case, different salting-out species were preferentially solvated in aqueous media leading to the liquid–liquid demixing. When dealing with high-charge density salts, with an enhanced capacity for creating hydration complexes, the formation of ABSs is more favourable for ILs with a weaker affinity for water, with more hydrophobic ILs being more easily excluded into a second liquid phase.[10,11,17–21] On the other side, when a moderately hydrophobic polymer, such as PPG-400,

and ILs are dissolved in aqueous media, the polymer molecules and the ions compete for the solvent molecules and also between themselves. Contrarily to what is observed in ABSs composed of ILs and high charge density salts,[10,11,17–21] in the present case, the competition is expected to be dominated by the IL anion that presents a higher ability to form hydration complexes. Based on this simplistic analysis, and on the observed reverse order of the IL anion effect compared to IL–salt ABSs, it would be reasonable to suggest a salting-out effect of the IL over PPG in aqueous media.[26–30,32] There are, however, when looking at the entire set of results currently available for both PEG and PPG, and from what is currently known on the nature of ILs in aqueous solution, a number of issues that cast doubts on this interpretation. Firstly, most ILs investigated to form polymer–IL ABSs are composed of salting-in inducing ions[26–30,32] and it is difficult to accept that they may be inducing a salting-out phenomenon. Yet, the major difficulty to reconcile is the observation made on this work in which anions less prone to accept protons than bromide and cations with alkyl chains longer than butyl are unable to induce ABS formation with PPG-400, unlike what was observed for PEGs of different molecular weights.[23,24] PEG being a more hydrophilic compound than PPG, it is unlikely that PEG is salted-out by $[CF_3SO_3]$-based ILs, or cations with hexyl or octyl alkyl chains, and PPG is not. This suggests that the IL salting-out mechanism proposed for the IL–PPG ABS formation[26–30,32] is not correct – results shown below for the IL cation further support this insight.

Based on our previous experience with PEG–IL ABSs, where it was found that a complex balance of interactions drives the ABS formation,[23,24] and on the results here reported for the various systems studied, that will be presented and discussed below, a mechanism of phase separation dominated by the interactions occurring between the IL and PPG, and that can be partly gauged from their mutual miscibilities, is here proposed. Given the higher hydrophobicity of PPG (compared for instance with PEG), ILs with longer alkyl side chains better interact with PPG through dispersive forces, while IL anions with higher hydrogen-bond basicity establish polar interactions with the ether and strong hydrogen-bonding interactions with terminal hydroxyl groups of the polymer. When these interactions between the IL and the polymer are more favourable than the interactions of the IL, or of PPG, with water, no ABS formation is observed. One of the main reasons behind the importance of polymer–IL interactions in the formation of ABSs is their low water content when compared, for instance, with systems formed by ILs and conventional salts. As a result, the interactions between the polymer and the IL become more important being further reflected in the ABS formation.

Zafarani-Moattar et al.[27] stated that PPG-400 is completely miscible with a highly concentrated aqueous solution of [C4mim]Br at temperatures close to room temperature. Considering that PPG-400 and [C4mim]Br are completely miscible in water, we can assume the formation of a type "0" ternary phase diagram. Following these considerations, we have performed additional experiments to evaluate if ILs totally miscible in PPG-400 form ternary phase diagrams of type "0". The formation of type "0"
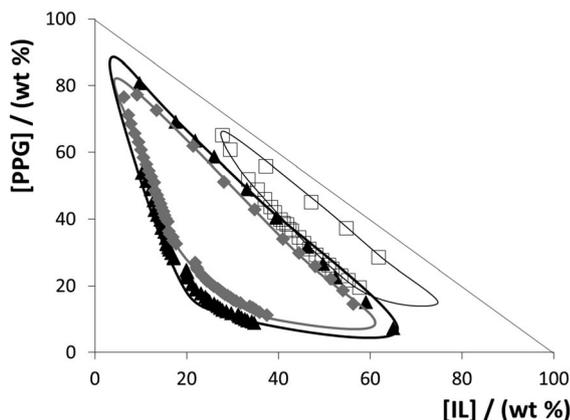
20574 | Phys. Chem. Chem. Phys., 2016, 18, 20571–20582

This journal is © the Owner Societies 2016

Fig. 2 Experimental type "0" ternary phase diagrams for ABSs composed of PPG-400 and [C$_4$mim]-based ILs at 298 K: □, [C$_4$mim][CH$_3$SO$_4$]; ◆, [C$_4$mim][CH$_3$CO$_2$]; ▲, [C$_4$mim][DMP]. The solid lines are only guidelines, in which the region inside of the lines corresponds to the biphasic regime.

Fig. 3 Binodal curves for ABSs composed of PPG-400 and chloride-based ILs at 298 K: ●, [C$_4$mim]Cl; ◇, [C$_4$mpy]Cl; ▲, [C$_4$mpip]Cl; ○, [C$_4$mpyr]Cl; ■, [Ch]Cl.

ternary phase diagrams was indeed confirmed for the systems composed of water, PPG-400 and [C$_4$mim][DMP], [C$_4$mim][CH$_3$CO$_2$] and [C$_4$mim][CH$_3$SO$_4$] – Fig. 2. Detailed data are given in the ESI.†

The appearance of the type "0" behaviour in ABSs (Fig. 2) is quite rare, and in the ABS domain almost exclusive for the polymer–IL type ABS,[34] since in more "traditional" ABSs composed of polymer–salt, salt–salt or polymer–polymer mixtures, one of the phase-forming agents shows limited solubility in water, or both phase-forming components exhibit a limited miscibility between themselves. Type "0" phase diagrams can be seen as interesting separation approaches since for a given IL concentration we can move from the monophasic–biphasic–monophasic regimes only by increasing the amount of PPG in the system, or *vice versa*.

Cation family effect

To assess the effect of the IL cation core on the formation of PPG-based ABSs, and to understand the interactions that occur at the molecular level, ternary phase diagrams were determined for a series of chloride-based ILs – depicted in Fig. 3. The aptitude of ILs to form ABSs follows the rank: [C$_4$mim]Cl < [C$_4$mpy]Cl < [C$_4$mpip]Cl < [C$_4$mpyr]Cl, whereas [N$_{4444}$]Cl and [P$_{4444}$]Cl are not able to form ABSs with PPG-400 at room temperature. This sequence correlates well with the relative hydrophobic character of each IL, based on their mutual solubilities with water,[41] but unlike the effect of the anion, now the non-aromatic, and most hydrophobic fluids, namely [C$_4$mpip]Cl and [C$_4$mpyr]Cl, produce the larger two-phase regions. This pattern is in stark contradiction to the trend observed with the anions and discussed above. In fact, no previous studies on the IL–PPG ABS were carried out addressing the IL cation effect, and thus, no conclusions were provided on this effect. Again, these results suggest that the proposed[26–30,32] salting-out mechanism of the IL over PPG for ABS formation is not correct. In the IL–salt ABS[14] there are no major differences between the aromatic and non-aromatic counterparts. It seems that the most important factor is the IL cation size, where 6-side ring cation ILs
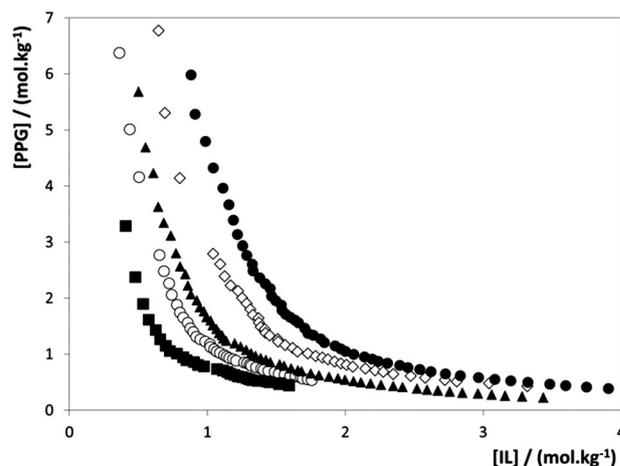
are more able to form ABSs with inorganic salts. The trend observed with PPG-based ABSs clearly supports the importance of the H-bonding ability of the IL cation with the polymer. The apparent contradiction with the results obtained for the aromatic *vs.* aliphatic cyclic cations, with the latter being able to form larger two-phase regions, is related to the enhanced interactions that the aromatic ring can establish with the ether group of the polymer, as shown by Tomé *et al.* using MD simulations.[33] Moreover, Li *et al.*[28] have also shown that polyethers are more soluble in ILs containing aromatic cations, such as imidazolium or pyridinium, due to enhanced hydrogen-bonding.

It is also shown that [P$_{4444}$]Cl and [N$_{4444}$]Cl are not able to form ABSs with PPG-400, although [P$_{4444}$]Cl forms two aqueous phases with PEG-2000.[24] In fact, tetrabutylphosphonium- and tetrabutylammonium-based ILs are two of the most hydrophobic compounds studied in this work, mainly due to the presence of four butyl chains. According to the model here proposed for ABS formation, the strong dispersive-type interactions that they can establish with PPG inhibit the phase separation and the ABS formation.

Cation alkyl chain length effect

The results illustrated in Fig. 4 allow the evaluation of the effect of the alkyl chain length of the IL cation on the ABS forming ability. While in the ABS of the type IL–salt an increase in the aliphatic chain enhances the formation of ABSs,[42] in polymer-based ABSs the opposite trend is observed. This contrary pattern was also observed with IL–PEG ABSs.[24] Along the homologous series of 1-alkyl-3-methylimidazolium chloride ILs, those with shorter alkyl chains are more able to form ABSs with PPG. The two-phase region decreases according to: [C$_1$mim]Cl > [C$_2$mim]Cl > [C$_3$mim]Cl ≫ [C$_4$C$_1$mim]Cl > [C$_4$mim]Cl, while ILs with alkyl chains longer than butyl, namely [C$_{5-7}$mim]Cl, are no longer capable of forming aqueous biphasic systems with PPG-400, as confirmed in this work, unlike what was observed with PEG for which ABSs were observed up to [C$_8$mim]Cl.[22] Again these results suggest that a salting-out mechanism of the IL over the polymer is not the
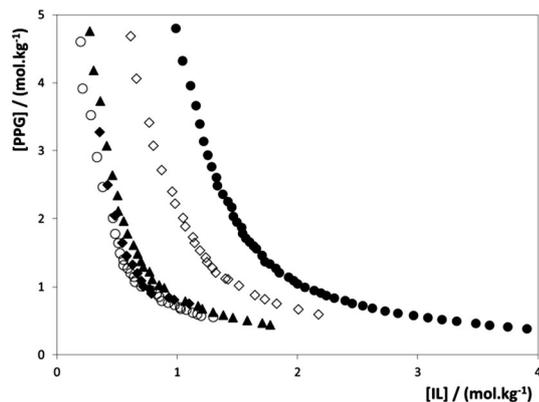
Fig. 4 Binodal curves for ABSs composed of PPG-400 and chloride-based ILs at 298 K: ●, [C₄mim]Cl; ◇, [C₄C₁mim]Cl. ▲, [C₃mim]Cl; ◆, [C₂mim]Cl; ○, [C₁mim]Cl.

driving force for the IL–PPG ABS formation. If [C₈mim]Cl were able to perform the salting-out of PEG, it would then be expected that it could be able to exert the same mechanism on the more hydrophobic PPG. However, no two-phase formation was observed in the PPG–IL–water systems. ILs with longer alkyl side chains enhance the hydrophobic character of the IL and, therefore, increase its affinity for PPG. In addition, the increase of the IL alkyl chain length leads to a decrease in the IL cation–anion interactions,[43] increasing therefore the availability of the cation and the anion to interact with the polymer.

Previous MD simulations aiming at understanding the influence of the alkyl chain length of the IL cation in the formation of PEG–IL-based ABSs showed that the phase separation is mainly controlled by the mutual solubilities between the polymer and the IL, being therefore a result of favourable/non-favourable interactions between the two species.[33] These hydrophobic interactions are almost negligible in systems composed of shorter aliphatic ILs (where polymer–IL association is mainly based on electrostatic interactions), but become more significant for ABSs comprising ILs with longer alkyl chains. Thus, the lower capacity to create a two-phase region seems to be related to the increase of the IL–polymer hydrophobic interactions.

The results obtained with [C₄C₁mim]Cl show that the replacement of the most acidic hydrogen at the cation expands the liquid–liquid immiscibility regime. Although an increase in the alkyl side chain length of disubstituted imidazolium-based ILs is not favourable for the creation of a second PPG-rich phase, [C₄C₁mim]Cl performs better than [C₄mim]Cl. [C₄C₁mim]Cl is a structural isomer of [C₅mim]Cl, which was not able to form ABSs with PPG-400. The elimination of the most acidic hydrogen at the imidazolium core has a huge influence on the phase diagram behaviour suggesting that the hydrogen bonding between the ether or hydroxyl groups of PPG and the most acidic proton on the imidazolium ring is a relevant factor. The presence of an "extra" methyl group instead of H in the position C2 at the IL cation decreases the ability for H-bonding interactions with PPG, and thus favours the formation of ABSs. This particular IL further supports the importance of hydrogen-bonding interactions occurring between PPG and ILs in addition to

dispersive-type interactions discussed before when analysing the cation alkyl side chain length effect. Watanabe and co-workers[40] demonstrated, with binary liquid–liquid equilibrium data, that the hydrogen-bonding between the oxygen atoms of polyethers and the aromatic hydrogen atoms at the IL cation plays an important role in the lower critical solution temperature (LCST) phase behaviour of these mixtures.[40] The substitution of the hydrogen atoms in the imidazolium ring by methyl groups resulted in lower LCST, i.e. decreases the polymer–IL mutual miscibility.[40] This pattern agrees well with the results obtained here for the phase behaviour of systems composed of [C₄mim]Cl and [C₄C₁mim]Cl.

Although it is demonstrated here that the mechanisms of phase separation in IL–PPG-based ABSs are mainly governed by the mutual IL–polymer interactions, there is no question that the salting-out effect is the dominant mechanism in IL–salt-based ABSs. The latter mechanism is easier to depict due to the high charge density of the salt ions with a high ability to be hydrated, and thus to act as salting-out species. However, there must exist transition regions between the two types of compounds (ILs versus salts) where the mechanism changes from the type here described to a salting-out phenomenon. This trend was indeed observed with [Ch]Cl. As shown in Fig. 3, the binodal for the system composed of [Ch]Cl displays the largest two-phase region, which can be attributed to its salt-like behaviour, dominated by Coulombic interactions and high ability to be hydrated, per opposition to ILs where polar and dispersive interactions dominate.

NMR analysis

To further investigate if the mechanisms governing the PEG–IL-based ABS previously reported[23,33,34] are related to those occurring in PPG–IL-based systems, three sets of ¹H NMR experiments were performed. To this end, the chemical shift deviations in PPG-400 and [C₄mim]Cl aqueous solutions, as a function of water, IL and PPG-400 concentrations, were determined (Fig. 5). The ¹H NMR measurements and chemical shift deviation calculations are presented in detail in the Experimental section while the chemical structure and atom numbering of the IL studied and PPG-400 are depicted in Fig. 5(a).

From all ¹H NMR chemical shift deviations displayed in Fig. 5, in general, strong positive deviations were not observed, i.e. deviations that support strong favourable interactions with the increase of the water, IL or PPG-400 concentrations. The first set of experiments, depicted in Fig. 5(a), in which the water was added to the PPG-400 + [C₄mim]Cl mixture, presents the more pronounced deviations. Interestingly, the increase of the water content does not affect the chemical shift environment of water and PPG protons (no significant deviations are observed). However, protons of the IL cation, in particular protons of the imidazolium ring (H(2), H(4), H(5) and H(6)), exhibit strong negative deviations. These results indicate that PPG–[C₄mim]⁺ interactions become less favourable with the increase of the water content. The behaviour that emerges from these results is that the interactions between PPG-400 and [C₄mim]Cl are less favourable with the increase of the water content in the ternary system, indicating a preferential solvation of both the IL
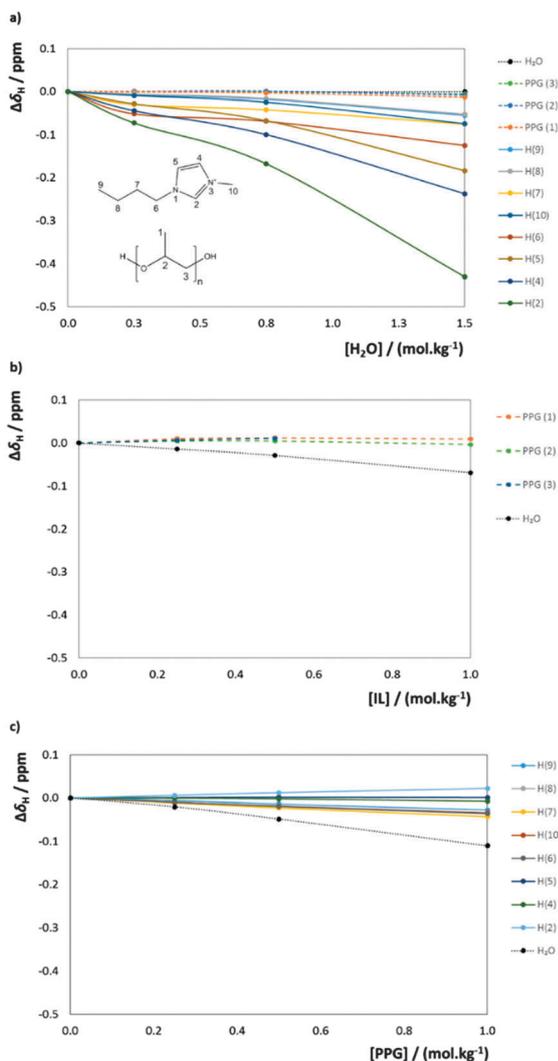
Fig. 5 ^{1}H NMR chemical shift deviations (at 298 K) as a function of water, [C$_4$mim]Cl and PPG-400 content: (a) PPG + IL binary mixture as a function of water molality; (b) PPG + water binary mixture as a function of [C$_4$mim]Cl molality; (c) IL + water binary mixture as a function of PPG-400 molality.

cation and the anion. This mechanism is further confirmed by an analysis of the second and third set of experiments (Fig. 5(b) and (c)). In both sets, the addition of the third component, respectively, IL and PPG-400, leads only to negative deviations of the water protons, demonstrating an increase of unfavourable interactions between PPG–water and IL–water when [C$_4$mim]Cl or PPG-400 is added, respectively. The increase of the [C$_4$mim]Cl concentration will disrupt the weak hydrogen bonding interactions occurring between water and the ether and terminal hydroxyl groups of the PPG polymer, maybe as a result of IL anion–water or PPG–IL interactions. A similar behaviour is the basis for the negative deviations observed in the chemical shifts of IL and water, where the addition of PPG-400 contributes to unfavourable interactions in the IL–water pairs, which are replaced by more favourable and stronger PPG-400–IL interactions.

From the ^{1}H NMR analysis it can be concluded that PPG–IL interactions become less favourable with the increase of water content. However, and as stated before, IL–polymer-based ABSs contain less water than IL–salt–ABSs, which is also a factor contributing to the predominant IL-polymer interactions which seem to govern their ABS forming ability.

COSMO-RS analysis

To complete the current analysis and to better interpret the experimental data, COSMO-RS was also used. To this end, the partition coefficient, log P, of the different ILs at infinite dilution between the PPG-400 and an aqueous phase was estimated. The log P has been reported previously as a reference quantitative parameter of the affinity between ILs and other compounds in aqueous solution.[44] Fig. 6 depicts the predicted log P values for all ILs studied. Fig. 6(a) shows the IL alkyl chain length effect, where an increase in the values of log P with the length of the alkyl chain is observed, *i.e.* [C$_1$mim]Cl has the strongest interaction with water and this interaction is weakened by increasing the length of the alkyl chain. Considering the ability to form ABSs with PPG-400, it was observed that ILs with highest log P values, as [C$_5$mim]Cl, [C$_6$mim]Cl and [C$_7$mim]Cl (hatched bars), are those that are not able to form ABSs, since they show a higher affinity towards PPG-400. Following the same description, Fig. 6(b) depicts the effect of the cation core and, in this case, the log P becomes positive to [N$_{4444}$]Cl and [P$_{4444}$]Cl, which were shown not to be able to form ABSs. These ILs present indeed higher partition coefficients which mean stronger interactions with PPG-400. Fig. 6(c) describes the IL anion effect and again the lowest values of log P were observed for those ILs that form ABSs (Cl-, Br-, [DMP]- and [CH$_3$SO$_4$]-based ILs). On the other hand, the positive or close to 0 values for log P are observed for the ILs that are not able to form ABSs with PPG-400. Therefore, COSMO-RS results confirm the molecular-level scenario described above based on experimental results: ILs with higher affinity or higher miscibility with PPG are those with a lower capacity to form ABSs. In addition, COSMO-RS results appear as *a priori* screening tools to predict the influence of the IL chemical structure and its ability (or not) to form ABSs with PPG-400.

Temperature dependency of ABS formation

In order to better understand the mechanisms which lead to liquid–liquid demixing, the effect of temperature on ABS formation was also addressed. The phase diagrams for [C$_4$mim]Cl, [C$_4$mim]Br and [C$_4$mim][DMP] at 298, 308 and 318 K are depicted in Fig. 7. For the studied systems, an increase in temperature enhances the immiscibility region. This pattern is in close agreement with previous works regarding conventional ABSs composed of PPG or PEG and salts[45,46] and other ABSs composed of imidazolium-[27] and cholinium-based[28] ILs and PPG-400. It is known that the intermolecular hydrogen-bonding between polyethers and imidazolium cations breaks at higher temperatures resulting in an easier phase separation of the binary mixture.[40] Therefore, the increased immiscibility between polymers and ILs at higher temperature translates into a higher ability to form ABSs.

This journal is © the Owner Societies 2016

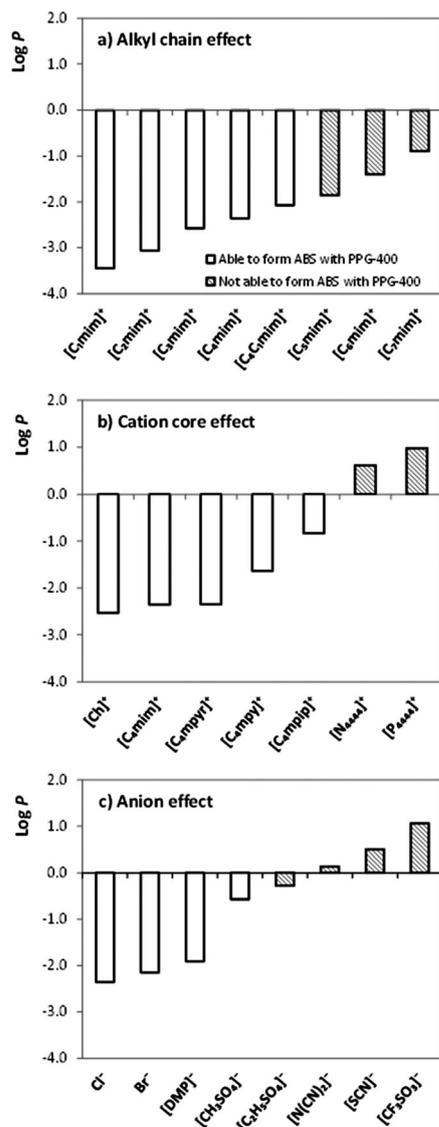*Phys. Chem. Chem. Phys.*, 2016, **18**, 20571–20582 | 20577

Fig. 6 Evaluation of the effect of (a) IL cation alkyl side chain length (using Cl-based ILs); (b) IL cation core (using Cl-based ILs); and (c) IL anion (using [C₄mim]-based ILs) in the logarithm of the partition coefficient of each IL between PPG-400 and water, predicted by COSMO-RS at 298 K.

The larger differences amongst the binodal curves at various temperatures for the chloride-based system relative to the [DMP]- and Br-based ABS are a direct result of stronger interactions occurring between the Cl-based IL and the polymer. Similar results were reported by Zafarani-Moattar et al.[27] for ABSs composed of PPG-400 and [C₂mim]Br and [C₄mim]Br. The binodal curve of the ABS composed of [C₂mim]Br is almost unaffected by the temperature whereas an increase in temperature favours the phase separation in the ABS formed by [C₄mim]Br.[27] As discussed before, ILs with longer aliphatic moieties present a higher mutual miscibility (or stronger interactions) with polymers which are further reflected in a stronger temperature effect on the phase diagrams.

Although the phase diagrams of Cl-based ABSs have a more pronounced dependence on temperature, it should be remarked
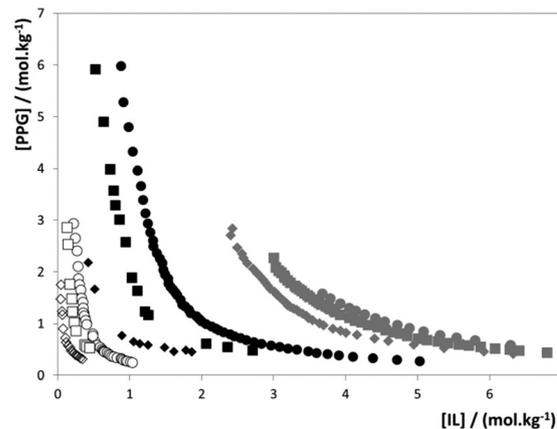

Fig. 7 Binodal curves for ABSs composed of PPG-400 and [C₄mim]Br (full grey symbols), [C₄mim]Cl (full black symbols) and [C₄mim][DMP] (open symbols) at: ●, ●, ○, 298 K; ■, ■, □, 308 K; ◆,◆, ◇, 318 K.

that this effect is still not so significant (for a 30 K temperature range) if compared with ABSs formed by protic ILs and PPG proposed before as remarkable thermoreversible systems,[47] where changes in 1 K are sufficient to trigger the phase separation for given mixture compositions. These IL-based ABSs were previously shown as significantly more versatile than classical liquid–liquid binary systems which are constrained by their critical temperatures.[47]

Chloranilic acid partitioning

The partitioning of chloroanilic acid was finally studied in the IL–PPG systems investigated. This molecule was used as a molecular probe of the coexisting phases' relative hydrophobicity. The molecular structure and the partition coefficients (K) of chloroanilic acid between the IL-rich and PPG-rich phases at 298 K are shown in Fig. 8. It is known that the partition of solutes between two phases depends on the relative compositions of the phases
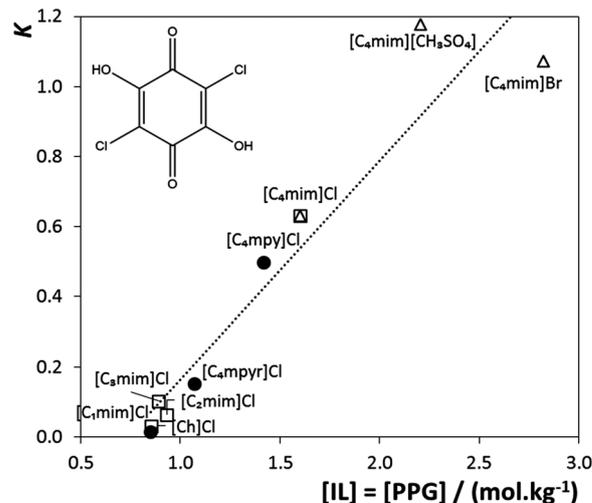

Fig. 8 Chemical structure of chloranilic acid and saturation solubility as a function of the partition coefficients at 298 K: ●, cation core effect; □, alkyl side chain length effect; △, anion nature effect.

20578 | *Phys. Chem. Chem. Phys.*, 2016, **18**, 20571–20582

This journal is © the Owner Societies 2016

and that the tie-line length (TLL) can be used to represent this difference. To avoid this effect, all partition studies were carried out at a fixed TLL, *circa* 90. The compositions of the coexisting phases at this TLL are presented in the ESI.† Moreover, all partition experiments were carried out at pH values lower than 1.0 to guarantee that the ''hydrophobic'' probe is present as a neutral molecule. The pK_a values of chloroanilic acid are 5.22 and 9.41 and correspond to the formation of the monovalent and divalent charged anions, respectively.[48] The conductivity and pH values of the coexisting phases are presented in the ESI.† The partition coefficients in systems formed by [C$_4$mim][DMP] and [C$_4$mim][CH$_3$CO$_2$] were not considered due to the speciation of these IL anions at the low pH values used in the partition study (pK_a of dimethyl hydrogen phosphate = 2.00 and pK_a of acetic acid = 4.54).[48] In fact, at this low pH value, we found that these ILs are no longer able to form ABSs with PPG-400 at 298 K.

In most systems the probe preferentially migrates to the PPG-rich phase. The octanol–water partition coefficient, K_{ow}, is a measure of the differential solubility of a neutral substance between two immiscible liquids, octanol and water, and thereby, it is a descriptor of the hydrophobicity of the probe. The log(K_{ow}) of chloroanilic acid is 1.22[48] meaning that the molecule tends to partition towards the more hydrophobic phase, in this case PPG.

Taking into account the binodal curves presented before, and assuming that the point at which the concentration of the IL equals the concentration of the polymer ([IL] = [PPG]) can be used as a measure of the liquid–liquid demixing aptitude, Fig. 8 shows that there is a linear correlation between this value and the partition coefficient of chloroanilic acid. Therefore, the hydrophobicity probe progressively migrates to the IL-rich phase as this phase becomes more hydrophobic, *i.e.* for phases composed of ILs with a lower ability to form ABSs with PPG-400. Independent of the IL cation core, the alkyl side chain length or anion nature, all results fall in a linear sequence showing that the relative hydrophobicity of the two phases can be easily tuned by an adequate selection of the IL.

With the large body of gathered experimental data here reported we can conclude that PPG–IL-based ABS formation is mainly ruled by IL–PPG interactions, and that the polarities of the coexisting phases can be manipulated by a suitable choice of the IL chemical structure.

Conclusions

In the present work, the mechanisms governing the formation of ABSs composed of PPG-400 and ILs were comprehensively investigated. Ternary phase diagrams of IL–PPG-400–water were determined at 298 K so that the effect of the IL structural features on the phase diagrams could be evaluated, namely the anion nature, the cation core and the cation alkyl side chain length. The effect of the temperature on the phase diagram behaviour was also addressed. It was observed that the higher the mutual miscibility or affinity between the IL and the polymer the more difficult it is to create the respective ABS. Moreover, an increase in temperature is favourable for the formation of IL–PPG ABSs.

Contrarily to systems composed of ILs and salts, where the ability of the ions to form hydration complexes mainly determines the liquid–liquid demixing ability, IL–PPG–water systems exhibit significant polymer–IL interactions that are dominant in the ABS formation. Experimental evidence was examined at a molecular level using ^{1}H NMR spectroscopy and COSMO-RS. A close correlation between the logarithm of the partition coefficient of the IL solute between the PPG-400 and the aqueous phase and their ability to form ABS was found, *i.e.* ILs which display a preferential partitioning to the PPG-rich phase are those that require a higher amount of polymer to undergo phase splitting in aqueous media. The complex nature of polymer–IL-based ABS formation and their tailoring ability on the phases' polarities was further shown by studies on the partitioning of a hydrophobic molecular dye. The partition coefficients obtained follow a linear trend with the ability of each IL to form an ABS.

Experimental

Materials

Polypropylene glycol with an average molecular weight of 400 g mol^{-1} (abbreviated as PPG-400) was acquired from Aldrich and was used as received. ILs investigated in this work were 1-butyl-3-methylimidazolium chloride ([C$_4$mim]Cl, 99 wt%), 1-butyl-3-methylimidazolium bromide ([C$_4$mim]Br, 99 wt%), 1-butyl-3-methylimidazolium dimethylphosphate ([C$_4$mim][DMP], 98 wt%), 1-butyl-3-methylimidazolium acetate ([C$_4$mim][CH$_3$CO$_2$], 98 wt%), 1-butyl-3-methylimidazolium methylsulphate ([C$_4$mim][CH$_3$SO$_4$], 99 wt%), 1-butyl-1-methylpiperidinium chloride ([C$_4$mpip]Cl, 99 wt%), 1-butyl-1-methylpyrrolidinium chloride ([C$_4$mpyr]Cl, 99 wt%), 1-butyl-3-methylpyridinium chloride ([C$_4$mpy]Cl, 98.0 wt%), 1,3-dimethylimidazolium chloride ([C$_1$mim]Cl), 1-ethyl-3-methylimidazolium chloride ([C$_2$mim]Cl, 98 wt%), 1-propyl-3-methylimidazolium chloride ([C$_3$mim]Cl, 98 wt%), 1-butyl-2,3-dimethylimidazolium chloride ([C$_4$C$_1$mim]Cl, 99.0 wt%), 1-butyl-3-methylimidazolium ethylsulphate ([C$_4$mim][C$_2$H$_5$SO$_4$], 98 wt%), 1-butyl-3-methylimidazolium trifluoromethanesulfonate ([C$_4$mim][CF$_3$SO$_3$], 99 wt%), 1-butyl-3-methylimidazolium dicyanamide ([C$_4$mim][N(CN)$_2$], 98 wt%), 1-butyl-3-methylimidazolium thiocyanate ([C$_4$mim][SCN], 98 wt%), 1-methyl-3-pentylimidazolium chloride ([C$_5$mim]Cl, 98 wt%), 1-hexyl-3-methylimidazolium chloride ([C$_6$mim]Cl, 98 wt%) and 1-heptyl-3-methylimidazolium chloride ([C$_7$mim]Cl, 98 wt%). These were purchased from Iolitec. Cholinium chloride ([Ch]Cl, 98 wt%) and tetrabutylammonium chloride ([N$_{4444}$]Cl, 97 wt%) were acquired from Sigma and tetrabutylphosphonium chloride ([P$_{4444}$]Cl, 97 wt%) was obtained from Cytec. Before use, all IL samples were dried under moderate temperature (343 K) and high vacuum conditions (<0.1 mbar) for a minimum of 48 h. The purity of each compound was additionally checked by ^{1}H and ^{13}C NMR and is in accordance with the purities given by the suppliers. The water content of all ILs and the polymer was measured by Karl-Fischer titration and was taken into account during the preparation of each aqueous solution. In general, the water content in all IL samples after the drying procedure was

This journal is © the Owner Societies 2016

Phys. Chem. Chem. Phys., 2016, **18**, 20571–20582 | **20579**

found to be <1000 ppm whereas the water content in the polymer was <10 000 ppm. For the NMR studies, deuterium oxide and 3-(trimethylsilyl)propionic-2,2,3,3-$d4$ acid sodium salt (TSP) were acquired from Aldrich with, respectively, >99.96% D atoms and >98% D atoms. Ultrapure water that was doubly distilled, passed through a reverse-osmosis system, and further treated with a Milli-Q plus water purification apparatus was used. Chloranilic acid (2,5-dichloro-3,6-dihydroxy-1,4-benzoquinone) used as a dye and the partitioning probe were from Merck. Hydrochloridric acid, at 37.0%, was from Riedel-de-Haën.

Phase diagrams

Aqueous solutions of PPG and aqueous solutions of different ILs at variable concentrations were prepared and used for the phase diagram determination. The ternary phase diagrams were determined at 298 (±1) K and at atmospheric pressure through the cloud point titration method.[17,18] Additional phase diagrams were determined at 308 and also at 318 (±1) K. The temperature was maintained by means of a double-jacketed cell coupled to a water bath circulator. Repetitive drop-wise addition of the IL aqueous solution to the PPG solution was carried out until the detection of a cloudy solution, *i.e.* the biphasic region, followed by the drop-wise addition of water until the establishment of a clear and limpid solution, *i.e.* the monophasic region. Drop-wise additions were carried out under constant stirring. Ternary system compositions were determined by weight quantification (±10^{-4} g) of all components added. The uncertainty associated to the weight fraction data of each phase diagram is below 0.8 wt%.

To determine the type "0" phase diagrams at 298 K the method proposed by Ruiz-Angel *et al.*,[49] and later adapted by Tomé *et al.*,[34] was used.

Partitioning of chloranilic acid

Specific mixture compositions within the two-phase region were selected and used to evaluate the chloranilic acid partitioning between the coexisting phases. The mixture compositions in all systems correspond to a TLL of 90. For each experiment, aqueous biphasic systems were prepared by mixing the exact amount of IL, polymer and an acidic aqueous solution. Chloranilic acid was added to the global mixture (*circa* 3 mg in a 5 g total mixture). The chloranilic acid is at a concentration low enough to be considered at infinite dilution and completely solvated in aqueous media, avoiding thus solute–solute interactions which could lead to different partitioning behaviours. HCl at 6 M was used as the aqueous phase aiming at achieving extremely acidic media (pH < 1.0). This acidification of the medium was carried out to guarantee that the dye is present as a neutral molecule and can act as a probe of the hydrophobicity of the coexisting phases.[50] After the complete dissolution of all components, the mixture was allowed to equilibrate for approximately 12 h and at 298 (±1) K. After the equilibration period, phases were carefully separated and weighted. The quantification of chloranilic acid was carried out in both phases by UV-Vis spectrophotometry using a SHIMADZU UV-1700, Pharma-Spec Spectrometer. Possible interferences of both the polymer and

the IL with the analytical method were taken into account and found to be of no significance at the dilutions carried out. The partition coefficient of chloranilic acid is defined as the ratio between the concentrations of the solute in the IL-rich phase and that in the PPG-rich phase.

NMR spectroscopy

For the ^{1}H NMR studies, three sets of experiments were performed: one for different IL molalities, one for different PPG molalities, and another one for varying the water concentration. For the first two sets, a solution of IL (or PPG) at approximately 1 mol kg^{-1} in D$_2$O, using TSP as a reference, was prepared gravimetrically with an associated uncertainty of ±10^{-4} g. The PPG (or IL) solutions were prepared gravimetrically in the D$_2$O–IL (or PPG) initial solution with PPG (or IL) concentrations ranging from 0 to 1 mol kg^{-1}. The ^{1}H NMR spectra were obtained for the initial D$_2$O–IL (or D$_2$O–PPG) solution and for the different ternary mixtures using a Bruker Avance 300 spectrometer operating at 300.13 MHz, with D$_2$O as solvent and TSP as internal reference. For the third set of experiments, a solution of IL at approximately 1 mol kg^{-1} in PPG was prepared gravimetrically with an associated uncertainty of ±10^{-4} g. The aqueous solutions were prepared gravimetrically in the IL–PPG initial solution with water molalities ranging from 0 to 1.5 mol kg^{-1}.

The ^{1}H NMR spectra were obtained for the initial PPG–IL solution and for the different ternary mixtures placed in NMR spectroscopy tubes containing sealed reference capillaries with D$_2$O and TSP as the internal reference, and at 298 K. For each set, the ^{1}H NMR chemical shift deviations were defined according to eqn (1)–(3), respectively:

$$\Delta\delta_H = \delta_H(\text{IL} + \text{PPG} + \text{D}_2\text{O}) - \delta_H(\text{IL} + \text{D}_2\text{O}) \quad (1)$$

$$\Delta\delta_H = \delta_H(\text{IL} + \text{PPG} + \text{D}_2\text{O}) - \delta_H(\text{PPG} + \text{D}_2\text{O}) \quad (2)$$

$$\Delta\delta_H = \delta_H(\text{IL} + \text{PPG} + \text{H}_2\text{O}) - \delta_H(\text{IL} + \text{PPG}) \quad (3)$$

where $\delta_H(\text{IL} + \text{PPG} + \text{D}_2\text{O})$ is the ^{1}H NMR chemical shift in the (IL + PPG + D$_2$O) solutions, $\delta_H(\text{IL} + \text{PPG} + \text{H}_2\text{O})$ is the ^{1}H NMR chemical shift in the (IL + PPG) aqueous solutions, and $\delta_H(\text{IL} + \text{D}_2\text{O})$, $\delta_H(\text{PPG} + \text{D}_2\text{O})$, and $\delta_H(\text{IL} + \text{PPG})$ are the ^{1}H NMR chemical shifts in the absence of PPG, IL, or water, respectively.

COSMO-RS

The molecular geometries of all compounds were optimized at the B3LYP/6-31++G* computational level in the ideal gas phase using the quantum chemical Gaussian 03 package,[51] describing the IL by an ion-pair structure, the aqueous media by individual water molecules and PPG-400 as a polymer with 5 units of the corresponding monomer. The ideal screening charges on the molecular surface for each species were calculated by the continuum solvation COSMO model using the BVP86/TZPV/DGA1 level of theory.[52] Subsequently, COSMO files were used as an input in the COSMOtherm code[53] to calculate the partition coefficient of each IL (log P) between PPG-400 and water at 298 K. The parameterization (BP_TZVP_C30_1201) was used.

20580 | *Phys. Chem. Chem. Phys.*, 2016, **18**, 20571–20582

This journal is © the Owner Societies 2016

Acknowledgements

Notes and references

1 R. D. Rogers and K. R. Seddon, *Science*, 2003, **302**, 792–793.

2 N. V. Plechkova and K. R. Seddon, *Chem. Soc. Rev.*, 2008, **37**, 123–150.

3 P. Wasserscheid and T. Welton, *Ionic Liquids in Synthesis*, Wiley-VCH Verlag GmbH & Co. KGaA, 2008.

4 J. P. Hallett and T. Welton, *Chem. Rev.*, 2011, **111**, 3508–3576.

5 C. F. Poole, *J. Chromatogr. A*, 2004, **1037**, 49–82.

6 X. Han and D. W. Armstrong, *Acc. Chem. Res.*, 2007, **40**, 1079–1086.

7 M. H. Abraham, A. M. Zissimos, J. G. Huddleston, H. D. Willauer, R. D. Rogers and W. E. Acree, *Ind. Eng. Chem. Res.*, 2003, **42**, 413–418.

8 A. F. M. Cláudio, L. Swift, J. P. Hallett, T. Welton, J. A. P. Coutinho and M. G. Freire, *Phys. Chem. Chem. Phys.*, 2014, **16**, 6593–6601.

9 M. A. Ab Rani, A. Brant, L. Crowhurst, A. Dolan, M. Lui, N. H. Hassan, J. P. Hallett, P. A. Hunt, H. Niedermeyer, J. M. Perez-Arlandis, M. Schrems, T. Welton and R. Wilding, *Phys. Chem. Chem. Phys.*, 2011, **13**, 16831–16840.

10 K. E. Gutowski, G. A. Broker, H. D. Willauer, J. G. Huddleston, R. P. Swatloski, J. D. Holbrey and R. D. Rogers, *J. Am. Chem. Soc.*, 2003, **125**, 6632–6633.

11 M. G. Freire, A. F. M. Cláudio, J. M. M. Araújo, J. A. P. Coutinho, I. M. Marrucho, J. N. C. Lopes and L. P. N. Rebelo, *Chem. Soc. Rev.*, 2012, **41**, 4966–4995.

12 P.-A. Albertsson, *Partition of Cell Particles and Macromolecules*, Wiley, New York, 3rd edn, 1986.

13 J. F. B. Pereira, L. P. N. Rebelo, R. D. Rogers, J. A. P. Coutinho and M. G. Freire, *Phys. Chem. Chem. Phys.*, 2013, **15**, 19580–19583.

14 S. Shahriari, L. C. Tomé, J. M. M. Araújo, L. P. N. Rebelo, J. A. P. Coutinho, I. M. Marrucho and M. G. Freire, *RSC Adv.*, 2013, **3**, 1835–1843.

15 Y. Pei, J. Wang, K. Wu, X. Xuan and X. Lu, *Sep. Purif. Technol.*, 2009, **64**, 288–295.

16 T. B. V. Dinis, H. Passos, D. L. D. Lima, V. I. Esteves, J. A. P. Coutinho and M. G. Freire, *Green Chem.*, 2015, **17**, 2570–2579.

17 C. M. S. S. Neves, S. P. M. Ventura, M. G. Freire, I. M. Marrucho and J. A. P. Coutinho, *J. Phys. Chem. B*, 2009, **113**, 5194–5199.

18 S. P. M. Ventura, C. M. S. S. Neves, M. G. Freire, I. M. Marrucho, J. Oliveira and J. A. P. Coutinho, *J. Phys. Chem. B*, 2009, **113**, 9304–9310.

19 F. J. Deive, A. Rodríguez, I. M. Marrucho and L. P. N. Rebelo, *J. Chem. Thermodyn.*, 2011, **43**, 1565–1572.

20 V. Najdanovic-Visak, J. N. C. Lopes, Z. P. Visak, J. Trindade and L. P. N. Rebelo, *Int. J. Mol. Sci.*, 2007, **8**, 736–748.

21 N. J. Bridges, K. E. Gutowski and R. D. Rogers, *Green Chem.*, 2007, **9**, 177–183.

22 S. Shahriari, C. M. S. S. Neves, M. G. Freire and J. A. P. Coutinho, *J. Phys. Chem. B*, 2012, **116**, 7252–7258.

23 J. F. B. Pereira, K. A. Kurnia, O. A. Cojocaru, G. Gurau, L. P. N. Rebelo, R. D. Rogers, M. G. Freire and J. A. P. Coutinho, *Phys. Chem. Chem. Phys.*, 2014, **16**, 5723–5731.

24 M. G. Freire, J. F. B. Pereira, M. Francisco, H. Rodríguez, L. P. N. Rebelo, R. D. Rogers and J. A. P. Coutinho, *Chem. – Eur. J.*, 2012, **18**, 1831–1839.

25 T. Mourão, L. C. Tomé, C. Florindo, L. P. N. Rebelo and I. M. Marrucho, *ACS Sustainable Chem. Eng.*, 2014, **2**, 2426–2434.

26 C. Wu, J. Wang, Y. Pei, H. Wang and Z. Li, *J. Chem. Eng. Data*, 2010, **55**, 5004–5008.

27 M. T. Zafarani-Moattar, S. Hamzehzadeh and S. Nasiri, *Biotechnol. Prog.*, 2012, **28**, 146–156.

28 Z. Li, X. Liu, Y. Pei, J. Wang and M. He, *Green Chem.*, 2012, **14**, 2941–2950.

29 X. Liu, Z. Li, Y. Pei, H. Wang and J. Wang, *J. Chem. Thermodyn.*, 2013, **60**, 1–8.

30 C. P. Song, R. N. Ramanan, R. Vijayaraghavan, D. R. MacFarlane, E. S. Chan and C. W. Ooi, *ACS Sustainable Chem. Eng.*, 2015, **3**, 3291–3298.

31 T. Moradian and R. Sadeghi, *J. Phys. Chem. B*, 2013, **117**, 7710–7717.

32 M. V. Quental, M. Caban, M. M. Pereira, P. Stepnowski, J. A. P. Coutinho and M. G. Freire, *Biotechnol. J.*, 2015, **10**, 1457–1466.

33 L. I. N. Tomé, J. F. B. Pereira, R. D. Rogers, M. G. Freire, J. R. B. Gomes and J. A. P. Coutinho, *J. Phys. Chem. B*, 2014, **118**, 4615–4629.

34 L. I. N. Tomé, J. F. B. Pereira, R. D. Rogers, M. G. Freire, J. R. B. Gomes and J. A. P. Coutinho, *Phys. Chem. Chem. Phys.*, 2014, **16**, 2271–2274.

35 A. Triolo, O. Russina, U. Keiderling and J. Kohlbrecher, *J. Phys. Chem. B*, 2006, **110**, 1513–1515.

36 H. Ohno, C. Suzuki, K. Fukumoto, M. Yoshizawa and K. Fujita, *Chem. Lett.*, 2003, **32**, 450–451.

37 A. Sarkar, S. Trivedi and S. Pandey, *J. Phys. Chem. B*, 2008, **112**, 9042–9049.

38 A. Sarkar, S. Trivedi and S. Pandey, *J. Phys. Chem. B*, 2009, **113**, 7606–7614.

39 J. F. B. Pereira, K. A. Kurnia, M. G. Freire, J. A. P. Coutinho and R. D. Rogers, *ChemPhysChem*, 2015, **16**, 2219–2225.

40 K. Kodama, R. Tsuda, K. Niitsuma, T. Tamura, T. Ueki, H. Kokubo and M. Watanabe, *Polym. J.*, 2011, **43**, 242–248.

41 M. G. Freire, P. J. Carvalho, A. M. S. Silva, L. M. N. B. F. Santos, L. P. N. Rebelo, I. M. Marrucho and J. A. P. Coutinho, *J. Phys. Chem. B*, 2009, **113**, 202–211.

42 M. G. Freire, C. M. S. S. Neves, J. N. Canongia Lopes, I. M. Marrucho, J. A. P. Coutinho and L. P. N. Rebelo, *J. Phys. Chem. B*, 2012, **116**, 7660–7668.

43 A. M. Fernandes, M. A. A. Rocha, M. G. Freire, I. M. Marrucho, J. A. P. Coutinho and L. M. N. B. F. Santos, *J. Phys. Chem. B*, 2011, **115**, 4033–4041.

44 J. Palomar, J. Lemus, M. A. Gilarranz and J. J. Rodriguez, *Carbon*, 2009, **47**, 1846–1856.

45 R. Sadeghi and B. Jamehbozorg, *Fluid Phase Equilib.*, 2009, **280**, 68–75.

46 R. Duraiayya, S. Arumugam and S. Settu, *J. Chem. Eng. Data*, 2012, **57**, 1112–1117.

47 H. Passos, A. Luís, J. A. P. Coutinho and M. G. Freire, *Sci. Rep.*, 2016, **6**, 20276.

48 ChemSpider, The free chemical database, http://www.chemspider.com/.

49 M. J. Ruiz-Angel, V. Pino, S. Carda-Broch and A. Berthod, *J. Chromatogr. A*, 2007, **1151**, 65–73.

50 S. I. Mostafa, *Transition Met. Chem.*, 1999, **24**, 306–310.

51 M. J. Frisch, G. W. Trucks, H. B. Schlegel, G. E. Scuseria, M. A. Robb, J. R. Cheeseman, J. A. Montgomery, Jr., T. Vreven, K. N. Kudin, J. C. Burant, J. M. Millam, S. S. Iyengar, J. Tomasi, V. Barone, B. Mennucci, M. Cossi, G. Scalmani, N. Rega, G. A. Petersson, H. Nakatsuji, M. Hada, M. Ehara, K. Toyota, R. Fukuda, J. Hasegawa, M. Ishida, T. Nakajima, Y. Honda, O. Kitao, H. Nakai, M. Klene, X. Li, J. E. Knox, H. P. Hratchian, J. B. Cross, V. Bakken, C. Adamo, J. Jaramillo, R. Gomperts, R. E. Stratmann, O. Yazyev, A. J. Austin, R. Cammi, C. Pomelli, J. W. Ochterski, P. Y. Ayala, K. Morokuma, G. A. Voth, P. Salvador, J. J. Dannenberg, V. G. Zakrzewski, S. Dapprich, A. D. Daniels, M. C. Strain, O. Farkas, D. K. Malick, A. D. Rabuck, K. Raghavachari, J. B. Foresman, J. V. Ortiz, Q. Cui, A. G. Baboul, S. Clifford, J. Cioslowski, B. B. Stefanov, G. Liu, A. Liashenko, P. Piskorz, I. Komaromi, R. L. Martin, D. J. Fox, T. Keith, M. A. Al-Laham, C. Y. Peng, A. Nanayakkara, M. Challacombe, P. M. W. Gill, B. Johnson, W. Chen, M. W. Wong, C. Gonzalez and J. A. Pople, *Gaussian 03, Revision C.02*, Gaussian Inc., Wallingford CT, 2004.

52 J. P. Perdew, *Phys. Rev. B: Condens. Matter Mater. Phys.*, 1986, **33**, 8822–8824.

53 COSMOtherm C2.1, release 01.06, Leverkusen, Germany: GmbH&GoKG, 2003.